WATER RESOURCES RESEARCH, VOL. 30, NO. 5, PAGES 1393–1405, MAY 1994

# Runoff simulation sensitivity to remotely sensed initial soil water content

D. C. Goodrich,[1] T. J. Schmugge,[2] T. J. Jackson,[2] C. L. Unkrich,[1]
T. O. Keefer,[1] R. Parry,[2] L. B. Bach,[3] and S. A. Amer[1]

**Abstract.** A variety of aircraft remotely sensed and conventional ground-based measurements of volumetric soil water content (SW) were made over two subwatersheds (4.4 and 631 ha) of the U.S. Department of Agriculture's Agricultural Research Service Walnut Gulch experimental watershed during the 1990 monsoon season. Spatially distributed soil water contents estimated remotely from the NASA push broom microwave radiometer (PBMR), an Institute of Radioengineering and Electronics (IRE) multifrequency radiometer, and three ground-based point methods were used to define prestorm initial SW for a distributed rainfall-runoff model (KINEROS; Woolhiser et al., 1990) at a small catchment scale (4.4 ha). At a medium catchment scale (631 ha or 6.31 $km^2$) spatially distributed PBMR SW data were aggregated via stream order reduction. The impacts of the various spatial averages of SW on runoff simulations are discussed and are compared to runoff simulations using SW estimates derived from a simple daily water balance model. It was found that at the small catchment scale the SW data obtained from any of the measurement methods could be used to obtain reasonable runoff predictions. At the medium catchment scale, a basin-wide remotely sensed average of initial water content was sufficient for runoff simulations. This has important implications for the possible use of satellite-based microwave soil moisture data to define prestorm SW because the low spatial resolutions of such sensors may not seriously impact runoff simulations under the conditions examined. However, at both the small and medium basin scale, adequate resources must be devoted to proper definition of the input rainfall to achieve reasonable runoff simulations.

## 1. Introduction

Passive microwave soil moisture research has focused on the basic questions involved in the data interpretation algorithm [*Jackson and Schmugge*, 1989]. There have been a number of efforts to develop water balance models that utilize these surface observations [*Jackson*, 1986; *Prevot et al.*, 1984]; however, these have only considered a single profile and have not considered surface runoff dynamics.

*Engman and Gurney* [1991] recently summarized some common viewpoints concerning remotely sensed soil moisture observations and hydrologic modeling. The general conclusion was that in order to fully utilize the information that frequent spatially distributed soil moisture observations might provide, we must reevaluate the hydrologic models themselves. The soil component of many existing models is constructed in such a way to make the model work even though soil moisture has never been available as an input variable. This element of the hydrologic cycle has thus become somewhat of a fitting parameter. As *Engman and Gurney* [1991] noted, actual observations of soil moisture may offer no improvement in runoff estimation because these models do not properly incorporate this variable. This was observed by *Jackson et al.* [1981] in a study involving a continuous runoff simulation model. In that study they examined how repetitive surface soil moisture observations could be used to calibrate and update a model. Errors resulting from inadequately defined spatial precipitation data could be corrected with surface soil moisture observations.

A study conducted by *Engman et al.* [1989] examined the impact of repetitive, spatially distributed remotely sensed soil moisture data on hydrologic modeling. Using a passive microwave data set collected in Kansas during the First International Satellite Land Surface Climatology Project Field Experiment (FIFE), the authors developed two-dimensional surface moisture maps. After a review of various modeling techniques, they selected a slab model developed by *Sloan and Moore* [1984]. They found that the observed soil moisture data provided an important check on model performance, feedback for the physical description of model elements, and information on the areas of the watershed contributing to base flow.

The Monsoon '90 interdisciplinary field experiment [*Kustas et al.*, 1991; *Kustas and Goodrich*, this issue] was conducted in the semiarid U.S. Department of Agriculture (USDA) Agricultural Research Service (ARS) Walnut Gulch experimental watershed in southeastern Arizona in which extensive rainfall and runoff data have been collected as part

[1]Southwest Watershed Research Center, Agricultural Research Service, U.S. Department of Agriculture, Tucson, Arizona.
[2]Hydrology Laboratory, Agricultural Research Service, U.S. Department of Agriculture, Beltsville, Maryland.
[3]Forest Service, U.S. Department of Agriculture, Pendleton, Oregon.



Paper number 93WR03083.

of a long-term research program [*Renard*, 1970]. The Monsoon '90 experiment provided a unique opportunity to utilize remotely sensed data for runoff estimation in an environment absent of base flow and dominated by ephemeral runoff. This contrasts with the study by *Engman et al.* [1989] in which the model applied was primarily structured to estimate more highly damped base flow watershed response.

The present study utilized a model (a research version of KINEROS [*Woolhiser et al.*, 1990]) which estimates Hortonian runoff on an event basis. The model is structured so that ground and remotely sensed estimates of soil water content can be directly utilized as input for the prestorm soil water content conditions. The model, with a variety of conventional ground-based as well as aircraft-based remotely sensed estimates of initial soil water contents, was applied to the brush-dominated [*Kincaid et al.*, 1964, 1966; *Daughtry et al.*, 1991] Lucky Hills–104 (LH-104) subwatershed at the small catchment scale (4.4 ha). At the medium scale of subwatershed WG11 (631 ha or 6.31 $km^2$) the model was also employed to estimate runoff using two-dimensional prestorm soil water content estimates obtained from the push broom microwave radiometer (PBMR) [*Schmugge et al.*, this issue]. The study was conducted with the following research objectives: (1) at the small catchment scale (4.4 ha), assess the utility of using a limited set of soil water content (SW) estimates, obtained from a variety of conventional ground-based and aircraft remote sensing methods, for distributed, event-based, rainfall-runoff computations and assess the sensitivity of the computations to the various SW estimates; (2) at the medium catchment scale (631 ha), assess the advantages of using distributed remotely sensed soil water content for definition of prestorm initial SW conditions for rainfall-runoff modeling; (3) at the medium catchment scale, compare runoff estimates obtained using remote estimates of SW to those obtained from a daily water balance model (a component of CREAMS [*Knisel*, 1980]) applied at the recording rain gages and interpolated across the catchment; and (4) at the medium catchment scale, assess the impact of aggregating spatially distributed remotely sensed estimates of SW on rainfall-runoff modeling.

## 2. Background

### 2.1. The Rainfall-Runoff Model (KINEROS)

The KINEROS user discretizes basin-contributing areas into one-dimensional overland flow and channel elements using topographic maps. Geometric, hydraulic, and soil parameters are either measured or estimated for each of the model elements. Because the model does not have an interstorm component, an estimate of the prestorm initial relative soil saturation (SI, denoting the fraction of pore space occupied by water) is required. The infiltration component of the model is based on the *Smith and Parlange* [1978] simplification of the Richards equation which assumes a semi-infinite, uniform soil for each model element. The Smith-Parlange model is stated as

$$f_c = K_s \frac{e^{F/B}}{(e^{F/B} - 1)} \tag{1}$$

$$B = G\varepsilon(S_{\max} - \mathrm{SI}) \tag{2}$$

where

$f_c$ infiltration capacity [$L/T$];
$F$ infiltrated water [$L$];
$K_s$ saturated hydraulic conductivity [$L/T$];
$G$ effective net capillary drive [$L$];
SW volumetric soil water content;
$S_{\max}$ maximum relative fillable porosity, equal to $\mathrm{SW}_{\max}/\varepsilon$;
SI initial relative soil saturation, equal to $\mathrm{SW}/\varepsilon$;
$\varepsilon$ porosity

In this formulation the suction term of the infiltration component is explicitly dependent upon the initial, prestorm volumetric water content. Significant sensitivity of the model runoff predictions to SI was demonstrated by *Goodrich* [1990]. Runoff generated by infiltration excess is routed interactively using kinematic wave equations on both overland flow and channel elements via a finite difference solution (see *Woolhiser et al.* [1990] for details). Interactive routing implies that infiltration and runoff are computed at each finite difference node considering rainfall, upstream inflow, and current degree of soil saturation. Therefore, unlike an excess routing scheme, infiltration can continue after rainfall ceases given that upstream inflow exists.

### 2.2. Data Collection

**2.2.1. Lucky Hills–104 (4.4 ha).** During the Monsoon '90 field campaign, volumetric soil water content, rainfall, and runoff were intensively monitored on the semiarid, brush-dominated LH-104 watershed from roughly July 23 to August 15, 1990. As part of the investigation, the small-scale spatial variability of rainfall in LH-104 was also monitored using five recording rain gages and 50 nonrecording rain gages [*Faurès*, 1990]. Runoff was measured at the outlet of the watershed by a calibrated Smith supercritical flume [*Smith et al.*, 1981].

Prestorm SW was measured by three ground-based methods and two remotely sensed methods. The ground-based methods were (1) gravimetric water content, converted to SW using bulk density measurements [*Schmugge et al.*, this issue]; (2) time domain reflectometry (TDR) [*Topp et al.*, 1980; *Zegelin et al.*, 1989; *Faurès*, 1990]; and (3) porous electrical resistance sensors (ERS) [*Coleman and Hendrix*, 1949; *Amer et al.*, 1994]. The gravimetric data (0–5 cm depth, average of three repetitions, roughly 0.3 m apart) were collected daily at approximately 9:30 A.M. adjacent to an automated meteorological and flux (METFLUX) station [*Kustas and Goodrich*, this issue] located approximately 190 m NNE of the centroid of watershed LH-104 (see Figure 1).

The TDR data were collected daily at approximately 9 A.M. at five locations adjacent to the recording rain gages within the LH-104 watershed separated by an average distance of 130 m (see Figure 1). An average value of these five readings was used as a measure of prestorm SW. The probes were 15 cm in length and were installed vertically from the surface to provide integrated volumetric water content over the top 15 cm of soil. In situ calibration was performed to develop a relationship between the TDR readings and SW.

The ERS were monitored every 20 min throughout the measurement period using a data logger located at the automated METFLUX station. The recorded resistance readings were converted to SW using laboratory calibration curves determined from soils obtained from the field site, along with in situ bulk density measurements [*Bradford and*

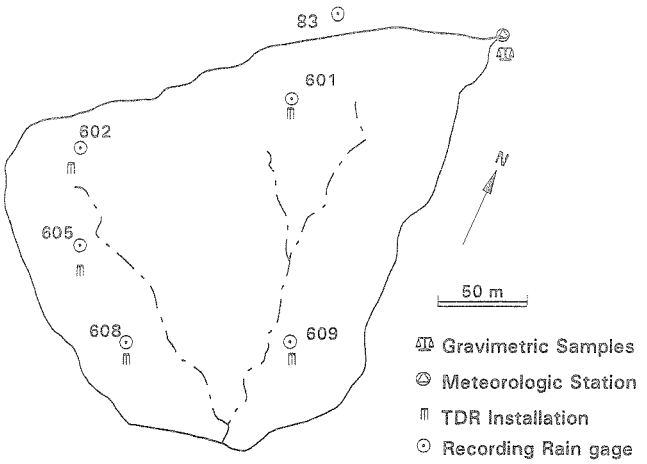


Figure 1. Lucky Hills–104 and ground soil water content measurement locations.

Table 1. Remotely Sensed Volumetric Soil Water Content and Acquisition Dates and Times for Lucky Hills Watershed 104

| | | IRE | | PBMR | |
|---|---|---|---|---|---|
| Date | DOY | Time | SW, % | Time | SW, % |
| July 31 | 212 | ... | ... | 1030 | 3.4 |
| Aug. 1 | 213 | ... | ... | ... | ... |
| Aug. 2 | 214 | 0830 | 13.7 | 0915 | 11.6 |
| Aug. 3 | 215 | 0830 | 11.4 | ... | ... |
| Aug. 4 | 216 | 0830 | 14.0 | 0830 | 12.7 |
| Aug. 5 | 217 | 0830 | 10.6 | 1000 | 7.4 |
| Aug. 6 | 218 | ... | ... | ... | ... |
| Aug. 7 | 219 | ... | ... | ... | ... |
| Aug. 8* | 220 | ... | ... | 0900 | 6.8 |
| Aug. 9 | 221 | ... | ... | 0900 | 4.5 |

*Partial watershed coverage only.

*Grossman*, 1982]. Three sensors were placed at a depth of 2.5 cm, roughly 0.5 m apart, and two at depth of 5 cm, roughly 0.5 m apart, and the average value of all five sensors was used to estimate prestorm SW. Economic and personnel constraints precluded obtaining distributed coverage of gravimetric and ERS measurements over the LH-104 watershed.

Remotely sensed estimates of SW were obtained from two instruments flown in fixed-wing aircraft. For both instruments the soil brightness temperature was measured, and after instrument verification, the surface soil water content was predicted using algorithms developed by USDA and the Institute of Radioengineering and Electronics (IRE) of the Academy of Sciences of the former USSR. The first instrument was a multifrequency microwave radiometer system (2.3, 21, and 27 cm wavelengths) provided by the IRE [*Jackson et al.*, 1992]. At the altitude flown (~150 m) this instrument provided an estimate of SW over a circular region approximately 105 m in diameter. Because the IRE radiometer operates only in profile mode and the flight line went through METFLUX station 1, the water content estimate centered over this station, adjacent to LH-104, was used for this study.

The second instrument was a push broom microwave radiometer (PBMR, 21 cm wavelength) operated by NASA [*Jackson et al.*, 1992; *Schmugge et al.*, this issue]. Multiple flight lines were flown with this instrument to obtain spatially distributed estimates of SW over the LH-104 watershed. Thirty-four PBMR pixels were extracted from the overflight data covering LH-104. Since the majority of the methods used to measure SW were point-based measurements, the 34 PBMR pixels were averaged to obtain a single value of SW for the LH-104 watershed. The effects of the spatial distribution of initial soil water content on runoff were more fully investigated within the larger WG11 watershed. The frequency of remotely sensed measurements was dependent upon aircraft availability; therefore temporal coverage during the experiment was not as extensive as for the ground-based methods, which were obtained at least daily. Table 1 contains the acquisition dates, times, and the average volumetric water content (SW) estimates for both the IRE ($n$ = 1 pixel) and PBMR ($n$ = 34 pixels) instruments (see section 3.1 for a discussion of the variability of the data).

Three rainfall events which caused runoff on LH-104 were observed during the field campaign with nearly simultaneous SW measurements. Table 2 contains the dates, starting times, average total rainfall depths based on the five recording rain gages (PPT), total observed runoff volume ($V$) and observed peak runoff rate ($Q_p$). Because of the stochastic nature of the storm arrival time, the infrequent gravimetric, TDR, PBMR, and IRE soil water content measurements must be adjusted to obtain values at the beginning of the storm. Since the electrical resistance sensor measurements were recorded every 20 min, the nearest point in time to storm onset was used, and no drying time adjustments were required. To perform the adjustment, daily TDR data at nine rain gage locations were analyzed during periods of drying to obtain an exponential decay function [*Faurès*, 1990]. The procedure also accounted for any intervening rain between measurement time and storm onset. However, very little intervening rainfall occurred. For the August 1 storm, approximately 1 mm of intervening precipitation occurred, resulting in adjustments to the initial SW ranging between 0.55 and 0.87%. Prior to the August 12 event, 2.3 mm of intervening rainfall occurred between the last IRE measurement and the storm, resulting in a 1.4% increase in SW. The volumetric soil water content (SW) was converted to initial

Table 2. Lucky Hills–104 and WG11 Runoff Events During the Monsoon '90 Campaign

| Date | DOY | Time* | PPT,† mm | $V$, mm | $Q_p$, mm/h |
|---|---|---|---|---|---|
| | | *LH-104 Basin* | | | |
| Aug. 1 | 213 | 1515 | 12.1 | 0.04 | 0.34 |
| Aug. 3 | 215 | 2040 | 13.3 | 3.5 | 17.5 |
| Aug. 12 | 224 | 0155 | 51.6 | 15.4 | 46.5 |
| | | *WG11 Basin* | | | |
| Aug. 1 | 213 | 1456 | 46.5 | 8.6 | 17.8 |
| Aug. 12 | 224 | 0200 | 30.4 | 0.42 | 0.72 |

*Earliest rain gage.
†Integrated over the watershed.

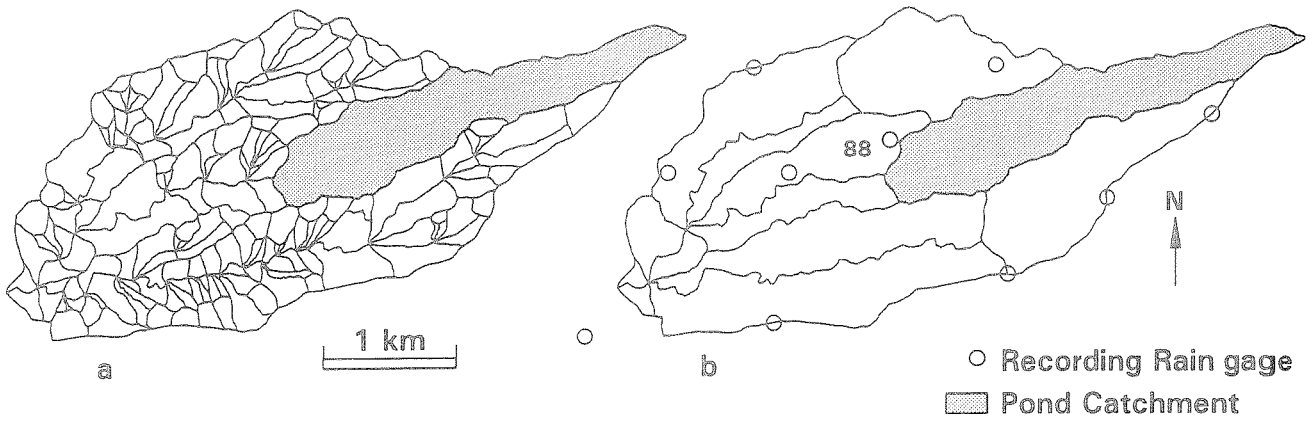


Figure 2. (a) Subwatershed WG11, discretized to 256 model elements. (b) Subwatershed WG11, discretized to 17 model elements.

relative soil saturation (SI) by dividing by a soil porosity of 0.394 (obtained from an average bulk density of 1.61, from 39 measurements in LH-104, and an assumed particle density of 2.65). The LH-104 basin average SI values from each measurement method were used for runoff model input. The time step employed for all LH-104 runs was 0.5 min. Implications for using these data in runoff modeling are presented in the discussion and analysis section.

**2.2.2. Subwatershed WG11 (631 ha, 6.31 km$^2$).** Subwatershed 11 (WG11) lies near the north central boundary of the USDA ARS Walnut Gulch experimental watershed and spans a transition in vegetation type from a semiarid shrub to grass. Ten recording rain gages are in or near this watershed and were used in subsequent analysis (see Figure 2). Runoff is measured at the watershed outlet with a Walnut Gulch supercritical flume [*Gwinn*, 1964]. In addition, two stock ponds are contained within this subwatershed. The area draining into these stock ponds was excluded from the analysis because the two runoff events under consideration had little (under 4%, August 1, 1990) or no (August 12, 1990) overflow volume from the ponds as compared to total runoff volume at the outlet. Table 2 also contains the start time of the rainfall (earliest of the ten rain gages), areal-averaged rainfall, runoff volume, and peak flow rate for these two WG11 events.

Areal estimates of SW over WG11 using the PBMR were obtained during the same flights used to obtain the LH-104 estimates for each of the dates and approximate times shown in Table 1 where full watershed coverage was available. A further analysis of these data is discussed in section 3.2. Calibration and georegistration information for the PBMR are described by *Schmugge et al.* [this issue]. With the data in this form it is possible to overlay the watershed boundaries and extract the appropriate data. The WG11 (631 ha) catchment was subdivided into 256 overland flow plane and channel model elements using 1:4800 orthophoto maps resulting in a mean overland flow element size of 3.42 ha and a mean first-order channel support area of 3.47 ha (Figure 2a). A geographic information system data layer consisting of boundary coordinates for each of the rainfall-runoff modeling element polygons was overlain onto the PBMR images. For each element the number of PBMR pixels and the average brightness temperature and soil water content as well as standard deviation were extracted for each of the PBMR overflights. Based on the analysis of *Schmugge et al.* [this issue], the brightness temperatures ($T_B$) in WG11 were transformed to volumetric soil water contents (SW, in percent) via the following linear transformation:

$$SW = -0.31(T_B) + 91.8 \quad (3)$$

This transformation was obtained from regression ($R^2$ of 0.94, standard error of estimate of 1.6%) between the gravimetric measurements at METFLUX site 4 and associated brightness temperatures of PBMR pixels in the vicinity of the METFLUX site. The same procedure used in LH-104 to adjust the SW to storm start times was employed in WG11 [*Faurès*, 1990]. The time-adjusted SW values were then divided by the soil porosity as obtained from texture via *Rawls et al.* [1982], to obtain SI (equation (2)). The entire upland portion of the WG11 watersheds has soils with a sandy loam texture (porosity, 0.45) and the channels are primarily sand (porosity, 0.44).

## 3. Discussion and Analysis

### 3.1. Small Catchment Scale: Lucky Hills–104 (4.4 ha)

Although a single spatial average of SI was used for KINEROS model input at the small LH-104 watershed scale, a brief discussion of the variability of SI across the sampling methods is presented to emphasize the scale dependence of each measurement method and enhance interpretation of the runoff modeling results. All soil water content estimation methods except the IRE resulted in multiple measurements within LH-104. The range and average SI from all five methods for four prestorm data collection periods (if available) are plotted in Figure 3. Note that drying time adjustment of SI to the prestorm point in time where event rainfall begins has not been performed in Figure 3 to highlight the variability encountered across measurement methods. For the four cases plotted, the maximum time between the various measurements, or sampling window, is roughly 2.5 hours. The variability illustrated in Figure 3 is typically a function of sampling scale, spatial measurement separation, and measurement error.

For example, the gravimetric and TDR measurements are separated by approximately 0.3 m and 130 m, respectively,

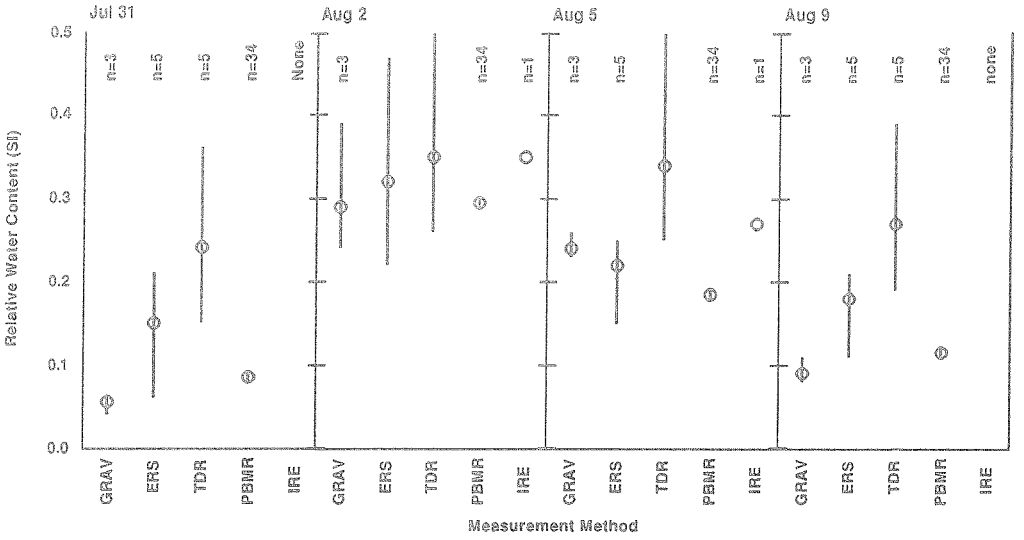


Figure 3. Average and range of SI by method for four data collection windows in LH-104.

whereas the spot diameter for all frequencies of the IRE is approximately 105 m (area roughly equal to 8700 $m^2$), and the spot diameter, or footprint, of each PBMR beam at a flight altitude of roughly 400 m is approximately 180 m. However, due to the rapid data sampling rates of the PBMR, the plane does not move a full 180 m before acquiring the next set of data. Therefore a great deal of pixel overlap exists. This is why 34 pixel samples are obtained in the relatively small LH-104 watershed. This contributes to the relatively small range of SI values for the PBMR data. In addition, these large-scale, remotely sensed spot samples integrate and average the SI over the small-scale heterogeneities caused by microtopography as well as textural and vegetal variation.

In contrast to the large-scale measurements, the ground-based methods (gravimetric, ERS, and TDR) sample a very small volume of soil (of the order of 100–300 $cm^3$). If the IRE instrument has a typical L band effective penetration depth of 2.0 cm, the IRE footprint will effectively sample a volume of soil roughly equal to $1.7 \times 10^8$ $cm^3$. The ground-based sampling methods are therefore much more likely to sample very small scale SI variations.

These data were used to estimate prestorm SI for input into the KINEROS rainfall-runoff model to address the first objective. *Goodrich* [1990] successfully calibrated and verified the KINEROS model on the Lucky Hills–104 (LH-104) watershed using observed rainfall at two recording rain gages and runoff data from 1973–1977 while assessing model performance using the Nash-Sutcliffe forecast coefficient of efficiency on runoff volume ($E_V$) and peak runoff rate ($E_Q$) for evaluation criteria [*Nash and Sutcliffe*, 1970]. The coefficient of efficiency was selected because it is dimensionless and is easily interpreted. If the model predicts observed runoff volume or peak runoff rate with perfection, $E_V$ or $E_Q$ would, respectively, equal 1. If $E < 0$, the model's predictive power is worse than simply using the average of observed values. The efficiency statistics reported by *Goodrich* [1990] for 16 independent verification events from the 1973–1977 time period on LH-104 were $E_V = 0.99$ and $E_Q = 0.96$.

The same calibrated input files describing the watershed geometry, soils, and hydraulic roughness were used in this investigation. However, it should be noted that since the calibration-verification time frame (1973–1977), a rain gage has been moved, the LH-104 runoff measuring structure has been changed (1978), and shrub to grass management manipulations have occurred on a portion of the watershed (approximately 1.8 ha, 1981 and 1984). Recalibration has not been undertaken because these manipulations continue to induce a period of nonstationary or changing watershed conditions.

For the events that occurred during the intensive 1990 field campaign the average prestorm SI values for each method and storm (prior to drying time adjustment these values correspond to SI values plotted as open circles in Figure 3) were input into KINEROS to assess the variability induced in computed runoff. To assess the relative magnitude of this variability, computer simulations were also conducted using different representations of the rainfall. This was accomplished by performing simulations with a single rain gage adjacent to LH-104 and contrasting them to the simulations made using the average SI values for the SI measurement method with the five recording rain gages used by *Faurès* [1990]. The research version of KINEROS used in this study employs a linear space-time rainfall interpolation scheme described by *Goodrich* [1990] to treat multiple rain gages. If a single rain gage is used, the rainfall field is considered uniform in space over the entire watershed.

Results from the simulations described above are summarized in Table 3. A cautionary note regarding interpretation of results regarding the LH-104 August 1 event is in order. This event was very small, and the total runoff volume on a per unit area basis was smaller than the measuring resolution of the recording rain gages. In this situation, instrument, data reduction, and observation errors are often a large part of the overall output signal and may dominate model response as measured by runoff quantities. Normally, an event whose runoff volume is smaller than one-half the rain gage measuring resolution is discarded for runoff simulation analysis, but it was included here because of the small number of events occurring during the intensive field campaign.

From Table 3 it is apparent that the model has a tendency

Table 3. Rainfall-Runoff Model Simulation Summary for Lucky Hills–104

| Water Content Method | August 1, 1990 | | | August 3, 1990 | | | August 12, 1990 | | |
|---|---|---|---|---|---|---|---|---|---|
| | SI | $V$, mm | $Q_p$, mm/h | SI | $V$, mm | $Q_p$, mm/h | SI | $V$, mm | $Q_p$, mm/h |
| GRAV | | | | | | | | | |
| Five gages | 0.05 | 0.01 | 0.03 | 0.22 | 2.2 | 10.8 | 0.06 | 18.1 | 58.7 |
| One gage | | 0.02 | 0.05 | | 2.7 | 17.0 | | 19.4 | 61.5 |
| ERS | | | | | | | | | |
| Five gages | 0.13 | 0.02 | 0.05 | 0.21 | 2.2 | 10.4 | 0.14 | 18.8 | 60.3 |
| One gage | | 0.03 | 0.10 | | 2.6 | 16.5 | | 20.1 | 63.3 |
| TDR | | | | | | | | | |
| Five gages | 0.22 | 0.04 | 0.10 | 0.31 | 2.6 | 12.8 | 0.22 | 19.5 | 61.9 |
| One gage | | 0.05 | 0.18 | | 3.1 | 19.6 | | 20.9 | 65.4 |
| PBMR | | | | | | | | | |
| Five gages | 0.08 | 0.02 | 0.03 | 0.29 | 2.5 | 12.2 | 0.10 | 18.4 | 59.3 |
| One gage | | 0.02 | 0.06 | | 3.0 | 19.0 | | 19.7 | 62.2 |
| IRE | | | | | | | | | |
| Five gages | ... | ... | ... | 0.29 | 2.5 | 12.3 | 0.20 | 19.1 | 61.5 |
| One gage | | ... | ... | | 3.0 | 19.1 | | 20.7 | 64.8 |
| Observed runoff | | 0.04 | 0.34 | | 3.5 | 17.5 | | 15.4 | 46.5 |

to underpredict the small event on August 1 and overpredict the large event of August 12. Previous comments regarding the model calibration and verification period and the subsequent watershed changes should be considered when comparing simulated to observed runoff data. In this part of the investigation the focus is on the variability induced in runoff simulations due to the variation in soil water content measuring method and changes in rainfall representation.

The variability in runoff volume and peak runoff rate induced by changes in relative soil water content measurement methods appears to be of the same order or smaller than that induced by using measured rainfall input from one instead of five rain gages (see Figure 1). To separate the effects of SI measurement method and rainfall representation more clearly, additional simulations were done holding the water content measuring method constant (TDR) and varying the model rainfall input by using each of the five recording rain gages individually for model input. This is contrasted with data from the five rain gage simulations presented in Table 3 in which the rainfall representation is held constant and the SI method changes. Figure 4 graphically summarizes these simulations. In this figure the range of measured 2-min peak rainfall intensities from each of the rain gages is used as a surrogate measure of rainfall variability among rain gages. This is an appropriate measure, as rainfall intensity largely controls runoff generation in the semiarid environment of LH-104.

The variability of SI and rainfall intensity should not be compared directly (incompatible measures) but can be interpreted via the induced variability in model outputs. In the middle two regions of Figure 4 the variability in runoff volume and the variability in peak rate in response to changes in the SI measurement method and changes in the rainfall representation are plotted side by side for each of the three runoff events. For comparison on an individual event basis the runoff simulation hydrographs and the observed hydrograph for the August 3, 1990, event are plotted in Figure 5. The hydrographs plotted in this figure illustrate the impact of using one and five rain gages with the gravimetric and IRE method. These data illustrate that the spatial variation in rainfall induces larger variations in runoff characteristics than the different SI measurement methods.

### 3.2. The Medium Catchment Scale: WG11 (6.31 km$^2$)

The WG11 catchment analysis is presented in separate subsections for clarity. Section 3.2.1 discusses the PBMR data and how they were used to estimate soil moisture for runoff simulations as well as the method of aggregating the PBMR data to address objectives 2 and 4. Section 3.2.2 briefly describes how prestorm soil moisture estimates derived from the CREAMS daily water balance model are incorporated into the runoff modeling effort to address objective 3. In section 3.2.3, comparative simulation analysis based on SI estimates from PBMR and CREAMS outlined in sections 3.2.1 and 3.2.2 is presented. Finally, in section 3.2.4 a description of the use of interesting historical rainfall patterns with 1990 PBMR-derived SI patterns to further explore PBMR aggregation impacts on runoff simulation is discussed.

**3.2.1. PBMR soil moisture estimates and runoff simulation method.** The distribution of PBMR-derived estimates of SI varied widely for the data acquisition dates listed in Table 1. The relative frequency distribution (counts per class over total counts) of all 40 × 40 m pixels in WG11 of PBMR-derived SI for each flight day (excluding day of year (DOY) 220 due to incomplete coverage) are reproduced in Figure 6. This figure qualitatively illustrates an apparent increase in the variability of SI with increasing mean SI. Further confirmation of this tendency is obtained by examining the variability across the 256 rainfall-runoff modeling elements. For each element a mean SI and standard deviation of SI were computed from the 40 × 40 m pixels falling within the element polygon (the average number of pixels per overland flow plane element equals 21). Using these data, the mean standard deviation of SI, computed across the 256 runoff model elements, is plotted against the mean of mean element SI for the same 256 model elements on the five flight days in Figure 7. Since SI, the relative initial water

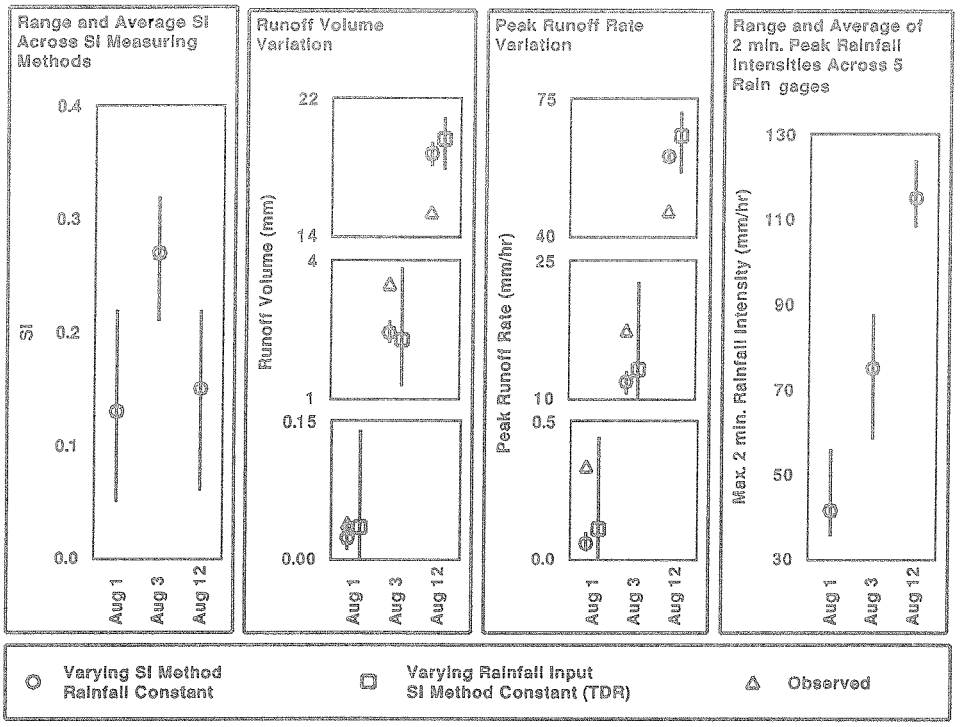


Figure 4. Variation in runoff volume and peak rate due to TDR SI variability and rainfall variability in LH-104.

content, is bounded by [0, 1] an entirely dry, uniform soil would have a theoretically uniform SI equal to the residual saturation with a standard deviation of zero. Similarly, for a totally saturated soil, SI would tend to one (or a maximum saturation under imbibition), and the standard deviation would tend to zero as indicated by the dashed line in Figure 7. Attaining a very high SI may not be realized given the rapid drainage in the coarse soils of WG11 and the difficulty of obtaining a PBMR flight immediately following an intense convective thunderstorm.

The impacts of averaging SI inputs on model runoff simulation should be most apparent in the region of maximum variability of SI. For the given data set this corresponds to the data acquired on DOY 214. Unfortunately, this is the day after the large runoff-producing event on DOY 213 (August 1, 1990). This was the reason for selection of historical storms for the analysis in section 3.2.3 to test hypothetical cases which should exhibit maximum interaction between the SI distribution and rainfall patterns in runoff production as interpreted through application of the KINEROS model.

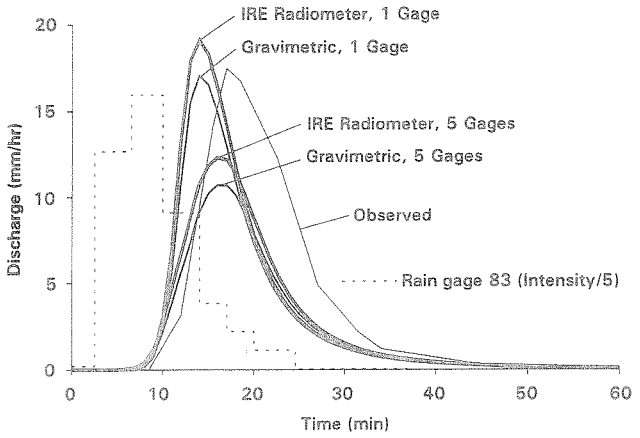


Figure 5. LH-104 observed and simulated hydrographs for August 3, 1990, event with different combinations of rain gage and SI model input.

Prior application of KINEROS to WG11 was conducted by *Goodrich* [1990]. In that study a split sample calibration and verification of events spanning a period of time from 1966 to 1988 was carried out using a research version of KINEROS. For 10 calibration events on WG11 the forecast coefficients of efficiency for runoff volume and peak runoff rate were $E_V = 0.86$ and $E_Q = 0.84$, respectively. For 20 independent verification events the efficiencies dropped off to $E_V = 0.49$ and $E_Q = 0.16$. Scatterplots of the observed versus simulated runoff volumes for the calibration and verification events set are presented in Figure 8.

The calibration efficiencies for WG11 were quite good when compared to other modeling studies with Walnut Gulch data [*Hughes and Beater*, 1989]. The scatterplots for the WG11 verification set (Figure 8) show a trend of underprediction for small events and overprediction for large events. If one believes the model does a fair job in representing the hydrologic response of WG11, this model representation can be utilized to assess the worth of the PBMR remotely sensed soil moisture estimates for runoff simulation. This constituted a basic premise of the study.

As in the case of the LH-104 watershed, the same calibrated input files describing catchment geometry, soils, and hydraulic roughness properties resulting from the prior calibration and verification of WG11 [*Goodrich*, 1990] were

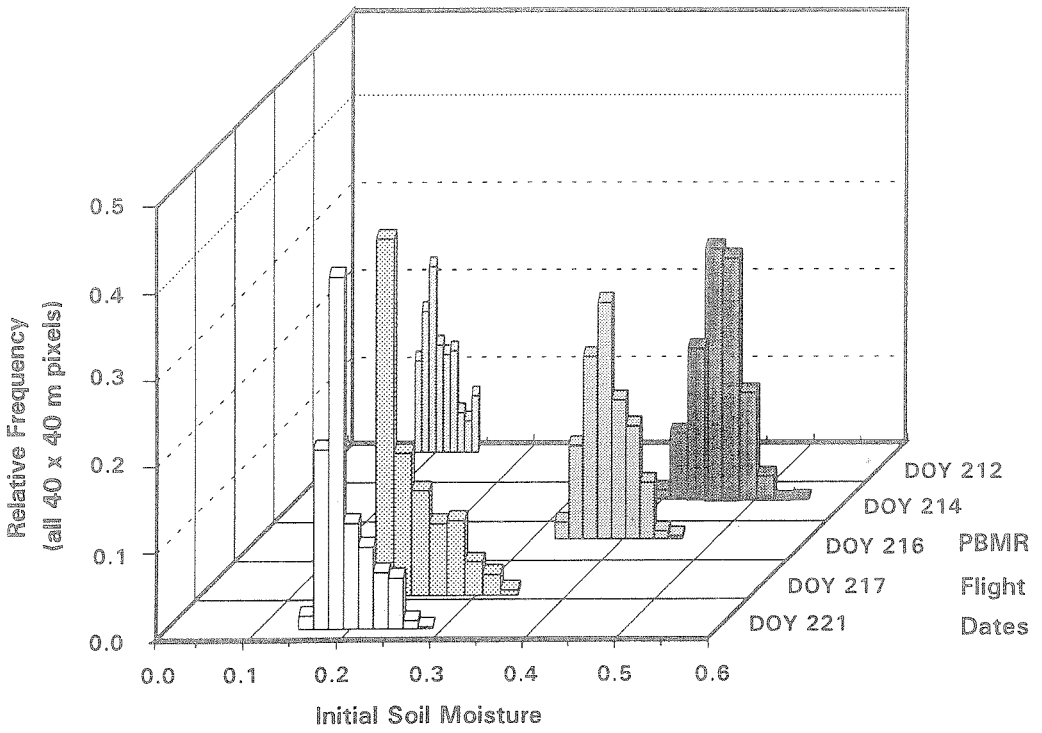


Figure 6. Relative frequency distribution of SI in WG11 derived from five PBMR flights.

used in this investigation. However, at the WG11 basin scale it was more realistic to examine the use of the areal distribution of remotely sensed prestorm initial relative soil water content (SI) measurements, and the aggregation of these measurements, on runoff simulations (objectives 2 and 4).

For each of the 256 runoff model elements (overland flow planes and channels) in Figure 2a, a mean prestorm SI derived from PBMR data was input to KINEROS for the August 1 and August 12 storm events. Breakpoint rainfall at each of the 10 rain gages was the other primary model input. As in the LH-104 analysis, the impacts on runoff simulation due to a simplified, uniform rainfall representation are assessed by using only rainfall input from a single centrally located rain gage in WG11 (rain gage 88, Figure 2b) with SI

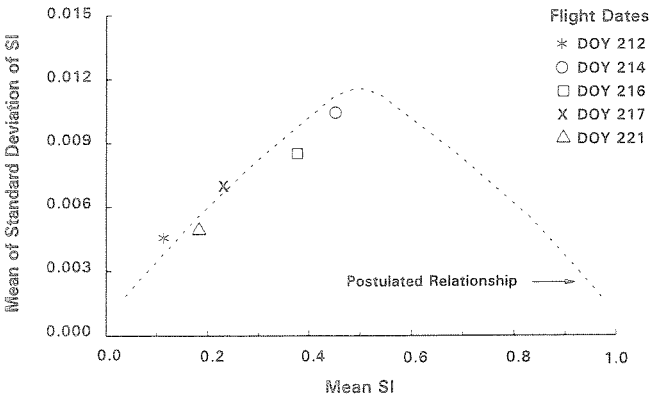


Figure 7. Mean runoff model element SI mean and mean element SI standard deviation. (SI values were computed from the 256-model element SI means and standard deviations; see Figure 2a.)

defined in the most complex manner, namely, 256 SI values, one for each rainfall-runoff model element.

To assess the impacts of averaging remotely sensed PBMR SI estimates on runoff model simulations, a stream order reduction methodology described by *Band* [1989] was utilized. This is a more logical approach of aggregation for assessing impacts on runoff modeling than pixel aggregation ($1 \times 1$ to $2 \times 2$, etc.) due to the directed nature of runoff generation imposed by the topography. In the first pass of this aggregation approach, the SI values are averaged using area weighting as if the first-order channels from the most complex basin representation (Figure 2a) are removed. This results in an effective stream order reduction of one for SI representation complexity. In the case of WG11 the number of independent SI values was reduced from 256 (Figure 2a) to 52 for the first aggregation (stream order reduction) step. In the next aggregation step the stream order for SI representation is reduced by one again, resulting in 17 (12 overland flow areas and five channels) independent SI inputs values per storm. This level of SI representation is shown in Figure 2b. During the averaging of the SI representation the topographic and geometric model complexity representations are not altered, so the impacts of SI averaging on runoff are isolated. Therefore 256 runoff model elements are maintained, but averaged SI values are assigned to groups of runoff model elements as the stream order averaging proceeds. The results of the various simulation runs are presented in section 3.2.3, where they are compared to the simulation runs using CREAMS SI estimates discussed in the next section.

**3.2.2. CREAMS soil moisture estimates and runoff simulation method.** To address objective 3, the utility of the remotely sensed PBMR SI estimates was judged by comparing these results to runoff simulations in which SI was

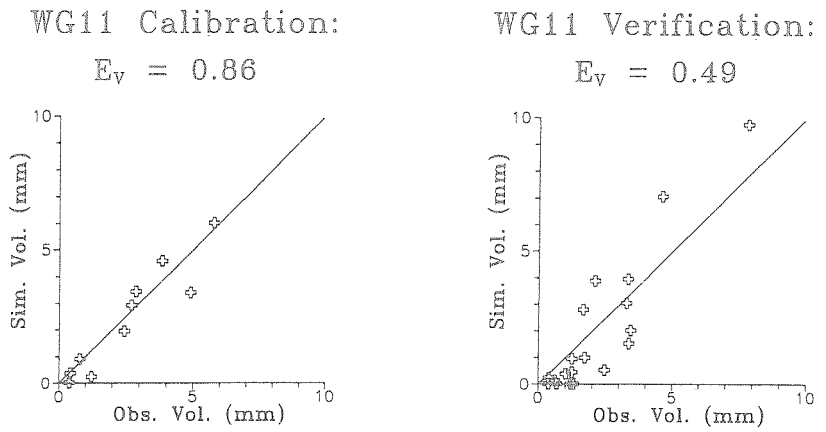


Figure 8. Observed versus simulated volumes for calibration and verification events sets for WG11.

obtained with a simple daily water balance model component of CREAMS [*Knisel et al.*, 1980]. CREAMS uses a daily time step to perform a multilayer soil water balance at the field scale. Input parameters are used to describe soil textural characteristics, plant rooting depth, and mean monthly changes in solar radiation, temperature, and leaf area index. Readers are referred to *Knisel et al.* [1980] for a more detailed description of CREAMS and related input parameters.

One of the primary inputs to CREAMS is daily rainfall depth for a given rain gage. Therefore SI values were computed on a rain gage by rain gage basis for each of the 10 rain gages used in the WG11 rainfall-runoff simulations. The CREAMS-derived SI estimates for each storm are interpolated to individual model runoff elements using a similar, but time-invariant, linear interpolation scheme as was used for rainfall interpolation [*Goodrich*, 1990]. Simulations for the August 1 and 12, 1990, events were completed using CREAMS-derived SI values. The results of these simulations are discussed and compared to the simulations using PBMR-derived SI estimates in the following section.

**3.2.3. Results and comparisons of runoff simulations using PBMR and CREAMS initial soil moisture estimates.** Distributed rainfall, prestorm time-adjusted PBMR and CREAMS estimates of SI, and locally generated total runoff per unit area (as interpolated from each model element) for the two SI input cases for the August 1, 1990, rainfall event are presented in Figure 9. It is apparent that the locally gener-

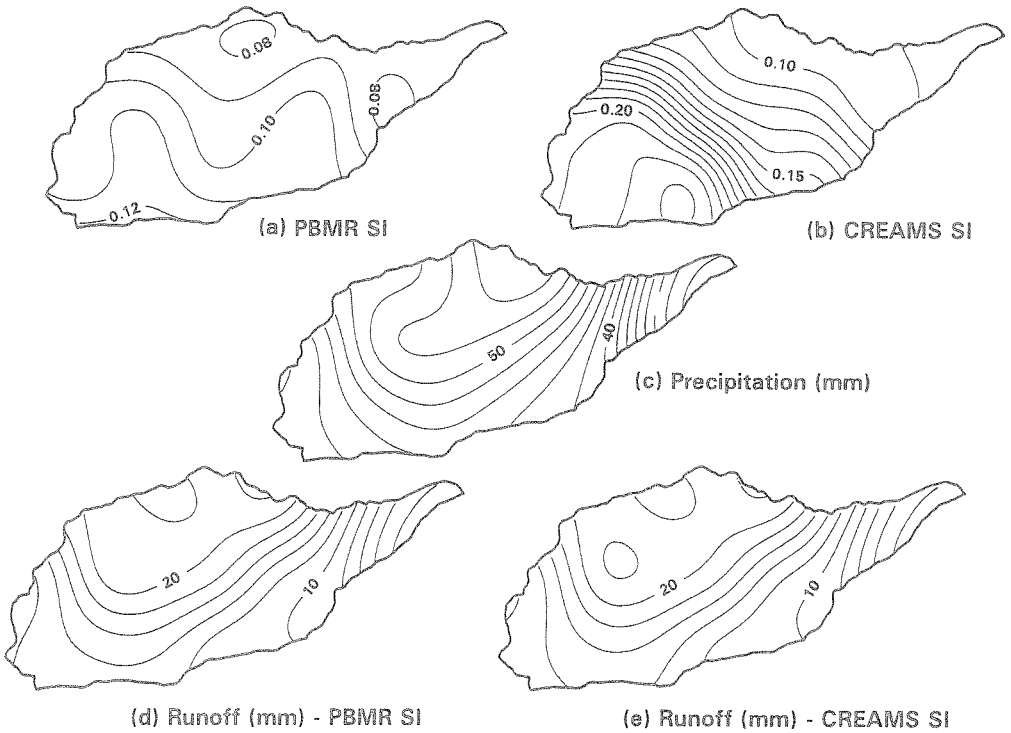


Figure 9. August 1, 1990, storm event: (a) PBMR SI estimates; (b) CREAMS SI estimates; (c) distributed precipitation (millimeters); (d) locally generated total runoff (millimeters) using PBMR SI inputs; (e) locally generated total runoff (millimeters) using CREAMS SI inputs.

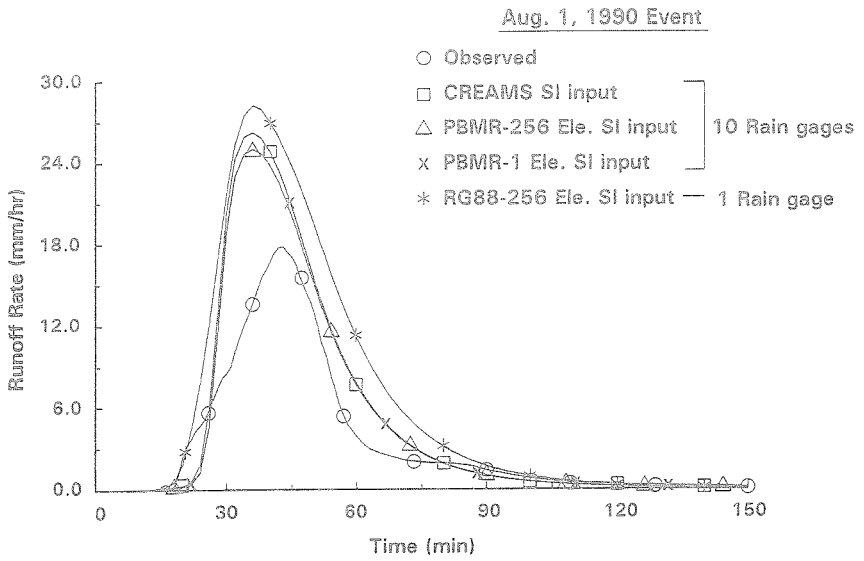


Figure 10. August 1, 1990, observed and simulated hydrographs.

ated total runoff from this storm for both SI input cases is largely dominated by the input rainfall pattern. Observed hydrographs and hydrographs of the various simulation combinations for the August 1 and 12 storm events are presented, respectively, in Figures 10 and 11. These figures include the simulated hydrographs for (1) CREAMS SI estimates with 10 rain gages, (2) PBMR SI estimates using 256 model elements and 10 rain gages, (3) PBMR SI estimates using one model element (a single basin average of SI) with 10 rain gages, and (4) PBMR SI estimates using 256 model elements and one central rain gage (number 88). The relative impact of different rainfall representations and PBMR SI averaging on total simulated runoff volume and peak runoff rate for the simulations illustrated in Figures 10 and 11 is summarized in Table 4.

The hydrographs plotted in Figures 10 and 11 indicate a general tendency of the model to overpredict the large event on August 1 and underpredict the smaller event on August 12. This is consistent with the verification results illustrated in Figure 8. No clear conclusion can be drawn on the relative advantage of using remotely sensed PBMR SI estimates or CREAMS SI estimates, as the PBMR SI inputs produce marginally better results for the August 1, 1990, storm but the situation is reversed for the August 12, 1990, storm. However, several conclusions can be drawn from Figures 10 and 11. As was the case in the small-catchment analysis on LH-104, the change in rainfall representation has a greater impact on runoff simulation than does a change in the SI input determination method from PBMR to CREAMS. This is readily apparent in the August 12, 1990, event and less so in the August 1, 1990, event. The other major conclusion that can be drawn from these figures is the minor impact of averaging of PBMR SI inputs on simulated runoff. The simulated hydrographs using 256 element SI inputs are

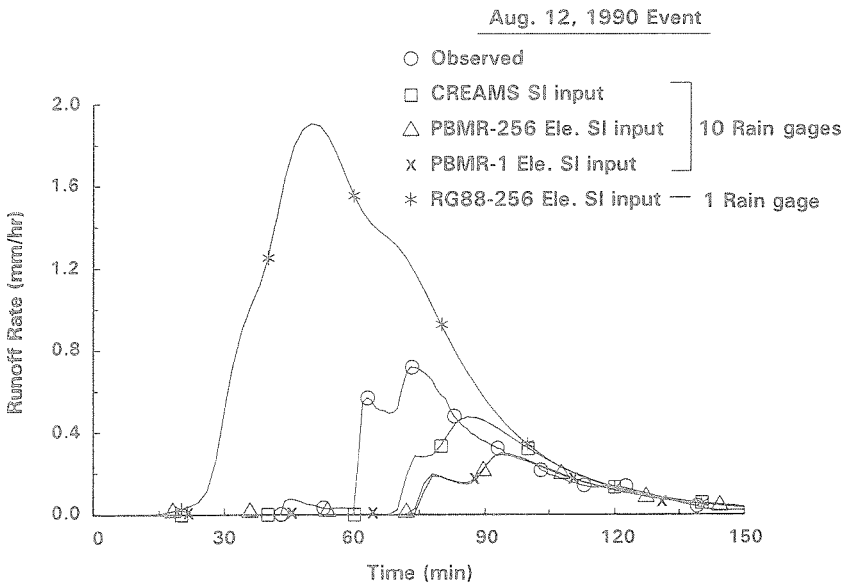


Figure 11. August 12, 1990, observed and simulated hydrographs.

virtually identical to those using a single basin-wide PBMR SI average.

The minor impacts on runoff simulation due to averaging PBMR SI inputs can be partially explained by the relatively uniform, dry initial conditions that existed prior to the observed runoff events on August 1 and 12 as illustrated in Figures 6 and 7. Impacts on runoff computations due to averaging of PBMR SI should be more apparent in a more variable, higher mean SI situation, as was alluded to earlier. This hypothesis is explored in the following section.

**3.2.4. PBMR SI aggregation impacts on runoff simulations using historical rainfall events.** To further investigate impacts of PBMR SI aggregation on runoff simulation, a hypothetical data set was assembled by assuming spatially distributed precipitation inputs from a variety of events fell on wetter, more variable, PBMR SI inputs from flights on August 2, 4, and 5, 1990 (see Table 1 and Figure 12) and were used as inputs into the KINEROS model. The rainfall events consisted of the August 1 and 12, 1990, storms as well as three historical storms (October 21, 1978; June 24, 1986; August 10, 1986). The rainfall events from the calibration set were selected for specific spatial rainfall patterns. The October 21, 1978, event was relatively uniform; the June 24, 1986, event had high rainfall gradients in the upper central portion of WG11; and the August 10, 1986, event produced steep precipitation gradients in the lower portion of WG11. Each of these events produced relatively small runoff events (October 21, 1978, $Q_p$ = 0.6 mm/h; June 24, 1986, $Q_p$ = 0.6 mm/h; and August 10, 1986, $Q_p$ = 2.5 mm/h) which will tend to maximize the influence of the SI initial conditions on runoff generation as the storm scale will not overwhelm the initial soil water content condition [*Goodrich*, 1990].

The averaging of PBMR SI patterns from the August 2, 4, and 5, 1990, flight dates, via the stream order reduction methodology described above, was repeated for each of these storms using 10 rain gages to describe rainfall input. The impacts of PBMR SI averaging on runoff simulation for these storm/SI combinations were then assessed. In addition, simulations using a single central rain gage, to describe rainfall input, were performed to compare the impacts of SI averaging against simplified rainfall representation. Figure 13 plots the absolute change in simulated peak runoff rate due to SI averaging (256 SI values to one) and a change in rainfall representation from 10 rain gages to one for each of the storm/SI combinations. Examination of this figure reveals that even with this varied range of storm and SI combinations, the impacts of using a single basin average of SI derived from PBMR are relatively small. In terms of an absolute percentage change in peak runoff rate the values ranged from 0.5% (June 24, 1986, storm, SI DOY 214) to 12.3% (August 10, 1986, storm, SI DOY 217) for SI averaging and 10.1% (August 1, 1990, storm, SI DOY 214) to over 400% (June 24, 1986, storm, SI DOY 217) for going from 10 rain gages to one rain gage, with the largest change occurring on the small historical runoff event. As was the case in the small catchment scale of the Lucky Hills–104 watershed (4.4 ha), differing spatial rainfall representation has a far greater impact than SI measurement on runoff simulations. It may be possible to better represent the spatial rainfall patterns using the PBMR brightness temperatures fields as a high correlation exists between these data and interpolated rainfall patterns [*Schmugge et al.*, this issue]. This subject is being addressed in subsequent analyses.

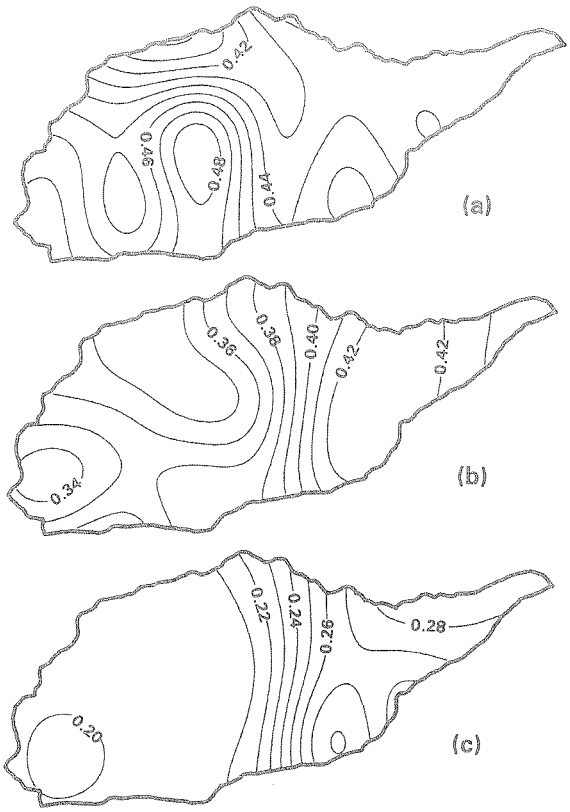


**Figure 12.** PBMR-derived SI patterns over WG11 for (a) August 2, 1990, (b) August 4, 1990, and (c) August 5, 1990 flights.

**Table 4.** WG11 Simulation Summaries for August 1 and August 12, 1990, Events

| Case | August 1, 1990 | | August 12, 1990 | |
|---|---|---|---|---|
| | $V$, mm | $Q_p$, mm/h | $V$, mm | $Q_p$, mm/h |
| Observed | 8.62 | 17.8 | 0.42 | 0.72 |
| 10 rain gages | | | | |
| CREAMS SI | 12.4 | 26.1 | 0.31 | 0.47 |
| PBMR SI, 256 elements | 11.8 | 24.9 | 0.20 | 0.30 |
| PBMR SI, 17 elements | 11.8 | 24.9 | 0.19 | 0.29 |
| PBMR SI, four elements | 11.9 | 25.0 | 0.20 | 0.29 |
| PBMR SI, one element | 11.9 | 25.0 | 0.20 | 0.29 |
| One rain gage (number 88): PBMR SI, 256 elements | 15.7 | 28.1 | 1.50 | 1.91 |

## 4. Conclusions

Conclusions regarding the analysis described in this investigation must be considered in the context of the semiarid Walnut Gulch environment, the small number of events considered, and the scale of water content measurement methods in relation to watershed scale. It should also be reiterated that runoff is almost exclusively generated via an infiltration excess mechanism in this environment. The con-

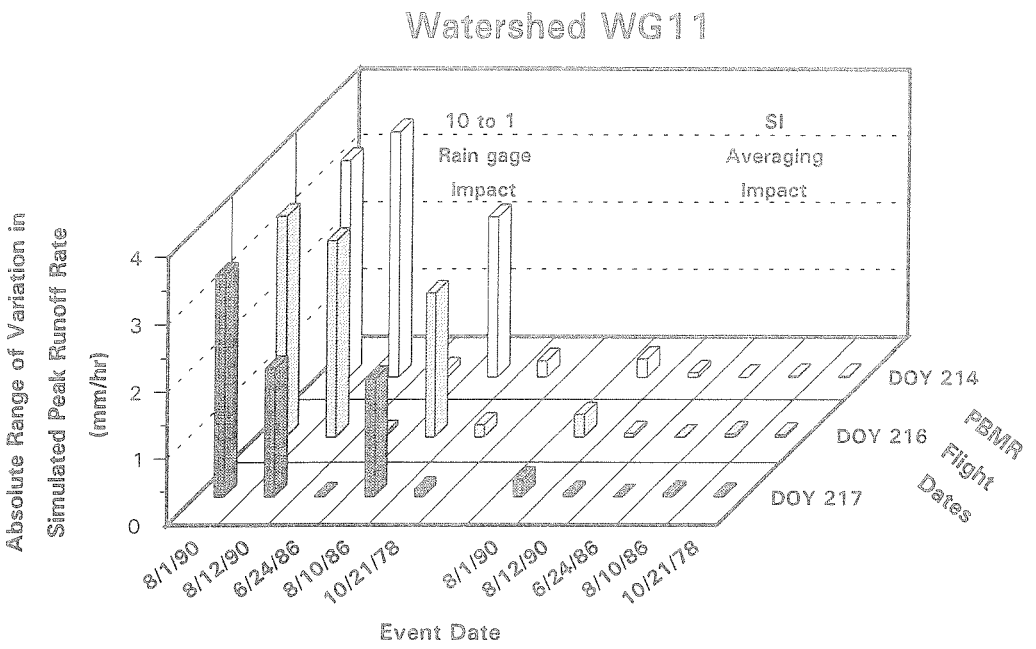


Figure 13. Impacts of PBMR SI averaging and rainfall representation on simulated peak runoff rate for various storm-SI combinations.

clusions are organized to address the objectives outlined earlier in the paper.

1. At the small watershed scale of Lucky Hills–104 (4.4 ha), when using an average value of SI for input, there appeared to be little difference among the SI measurement methods as indicated by the variation in computed runoff volume and peak rate. If an average value of initial relative water content (SI) value is desired for runoff modeling, it could be reasonably obtained by any of the methods used in the study. However, changes in rainfall representation had a much greater impact on runoff simulation than changes in SI input determination, so adequate resources should be devoted to definition of spatial rainfall variability.

2. Remotely sensed estimates of distributed prestorm initial soil water content were easily integrated as input into the KINEROS rainfall-runoff model at the medium catchment scale (6.31 $km^2$). This required georeferenced brightness temperature estimates and transformation equations to convert brightness temperature to volumetric soil water content [*Schmugge et al.*, this issue]. The infiltration formulation in KINEROS can directly incorporate information in this form after an adjustment is made for surface drying in the elapsed time between the flight and the beginning of runoff-producing rainfall.

3. Based on this data set, it appears that the CREAMS SI estimation method works as well as the remotely sensed SI estimation method. Though the differences between the spatially distributed SI patterns from CREAMS and PBMR appeared to be substantial (Figures 9a and 9b), the influence on runoff model output was small. This does not imply that for another process, such as evapotranspiration modeling and estimation, one or the other method will be advantageous.

4. For runoff simulations a simple basin average of remotely derived SI estimates at the medium catchment scale (631 ha or 6.31 $km^2$) appears to be adequate for runoff simulation. However, as was the case at the small catchment scale (4.4 ha), a greater spatial resolution of the rainfall is required, and adequate resources should be devoted to this task. This result has important implications for the use of space-based microwave estimates for defining distributed prestorm initial soil water content conditions for rainfall-runoff modeling in semiarid regions. A criticism of typical passive microwave sensors is their relatively coarse spatial resolution. This analysis indicates that using a single basin average of SI for the 6.31 $km^2$ WG11 basin does not seriously limit use of such data for rainfall-runoff modeling for the test cases examined. Therefore for deriving prestorm soil water content conditions for runoff modeling, satellite-based passive microwave systems may be entirely adequate (current technology, depending on antenna size and orbital altitude, enables resolutions of between 5 and 10 km). However, analysis at yet larger scales is warranted, and until comparable data collection and analysis is performed in other diverse situations, this conclusion must, of course, be limited to the semiarid conditions examined. The conclusions must also be tempered by understanding that using the KINEROS rainfall-runoff model carries with it associated assumptions in its formulation and implementation. The primary focus of this study concentrated on runoff processes, and extrapolation of the conclusions to other processes is not warranted. Definition of resolution requirements for other processes, such as the estimation and simulation of energy fluxes and evapotranspiration using parallel analysis, is an immediate and important task. This task is the subject of ongoing research using the Walnut Gulch and Monsoon '90 databases.

**Acknowledgments.** This study would not have been possible without the dedication of the USDA ARS Southwest Watershed Research Center which provided financial support in development and maintenance of the long-term research facilities in Tucson and

Tombstone, Arizona. Special thanks is extended to the staff located in Tombstone, Arizona, for their continued efforts. Support for this effort was provided by USDA ARS, and in part by the NASA Interdisciplinary Research Program in Earth Sciences (NASA reference number IDP-88-086), by grant I-1486-88 from BARD, the United States–Israel Binational Agricultural Research and Development Fund, and the NASA/EOS grant NAGW2425. This assistance is gratefully acknowledged. The authors would also like to thank two anonymous reviewers for thorough reviews and helpful suggestions.

## References

Amer, S. A., T. O. Keefer, M. A. Weltz, D. C. Goodrich, and L. B. Bach, Soil moisture sensors for continuous monitoring, *Water Resour. Bull.*, in press, 1994.

Band, L. E., A terrain-based watershed information system, *Hydrol. Processes*, *4*, 151–162, 1989.

Bradford, J. M., and R. B. Grossman, In-situ measurement of near surface soil strength by the full cone device, *Soil Sci. Soc. Am. J.*, *46*, 685–688, 1982.

Coleman, E. A., and T. M. Hendrix, Fiberglass electrical soil-moisture instrument, *Soil Sci.*, *67*, 425–438, 1949.

Daughtry, C. S. T., M. A. Weltz, E. M. Perry, and W. P. Dulaney, Direct and indirect estimates of leaf area index, paper presented at the special session on hydrometeorology, 20th Conference on Agriculture and Forest Meteorology, Am. Meteorol. Soc., Salt Lake City, Utah, Sept. 10–13, 1991.

Engman, E. T., and R. J. Gurney, *Remote Sensing in Hydrology*, Chapman and Hall, London, 1991.

Engman, E. T., G. Angus, and W. P. Kustas, Relationships between the hydrologic balance of a small watershed and remotely sensed soil moisture, in Remote Sensing and Large-Scale Global Processes, *IAHS Publ.*, *186*, 75–84, 1989.

Faurès, J. M., Sensitivity of runoff to small scale spatial variability of observed rainfall in a distributed model, M.S. thesis, 169 pp., Univ. of Ariz., Tucson, 1990.

Goodrich, D. C., Geometric simplification of a distributed rainfall-runoff model over a range of basin scales, Ph.D. dissertation, 361 pp., Univ. of Ariz., Tucson, 1990.

Gwinn, W. R., Walnut Gulch supercritical measuring flume, *Trans. ASAE*, *7*(3), 197–199, 1964.

Hughes, D. A., and A. B. Beater, The applicability of two single event models to catchments with different physical characteristics, *Hydrol. Sci. J.*, *34*(1,2), 63–78, 1989.

Jackson, T. J., Soil water modeling and remote sensing, *IEEE Trans. Geosci. Remote Sens.*, *GE-24*(1), 37–46, 1986.

Jackson, T. J., and T. J. Schmugge, Passive microwave remote sensing system for soil moisture: Some supporting research, *IEEE Trans. Geosci. Remote Sens.*, *GE-27*(2), 225–235, 1989.

Jackson, T. J., T. J. Schmugge, A. D. Nicks, G. A. Coleman, and E. T. Engman, Soil moisture updating and microwave remote sensing for hydrologic simulation, *Hydrol. Sci. Bull.*, *26*(3), 305–319, 1981.

Jackson, T. J., et al., Multifrequency passive microwave observations of soil moisture in an arid rangeland environment, *Int. J. Remote Sens.*, *13*(3), 573–580, 1992.

Kincaid, D. R., J. L. Gardner, and H. A. Schreiber, Soil and vegetation parameters affecting infiltration under semiarid conditions, *IASH Publ.*, *65*, 440–453, 1964.

Kincaid, D. R., H. B. Osborn, J. L. Gardner, Use of unit-source watersheds for hydrologic investigations in the semiarid southwest, *Water Resour. Res.*, *2*(3), 381–392, 1966.

Knisel, W. G. (Ed.), CREAMS: A field scale model for chemicals, runoff, and erosion from agricultural management systems, *Conserv. Res. Rep. 26*, 643 pp., Sci. and Educ. Admin., U.S. Dep. of Agric., Washington, D. C., 1980.

Kustas, W. P., et al., An interdisciplinary field study of the energy and water fluxes in the atmosphere-biosphere system over semi-arid rangelands: Description and some preliminary results, *Bull. Am. Meteorol. Soc.*, *72*(11), 1683–1706, 1991.

Kustas, W. P., and D. C. Goodrich, Preface, *Water Resour. Res.*, this issue.

Nash, J. E., and J. V. Sutcliffe, River flow forecasting through conceptual models, I, A discussion of principles, *J. Hydrol.*, *10*, 282–290, 1970.

Prevot, L., R. Bernard, O. Taconet, D. Vidal-Madjar, and J. L. Thony, Evaporation from a bare soil evaluated using a soil water transfer model and remotely sensed surface soil moisture data, *Water Resour. Res.*, *20*(2), 311–316, 1984.

Rawls, W. J., D. L. Brakensiek, and K. E. Saxton, Estimation of soil water properties, *Trans. ASAE*, *25*, 1316–1320, 1328, 1982.

Renard, K. G., The hydrology of semiarid rangeland watersheds, *Rep. 41-162*, 26 pp., Agric. Res. Serv., U.S. Dep. of Agric., Washington, D. C., 1970.

Schmugge, T., T. J. Jackson, W. P. Kustas, R. Roberts, R. Parry, D. C. Goodrich, S. A. Amer, and M. A. Weltz, Push broom microwave radiometer observations of surface soil moisture in Monsoon '90, *Water Resour. Res.*, this issue.

Sloan, P. G., and I. D. Moore, Modeling subsurface stormflow on steeply sloping forested watersheds, *Water Resour. Res.*, *20*(12), 1815–1822, 1984.

Smith, R. E., and J.-Y. Parlange, A parameter-efficient hydrologic infiltration model, *Water Resour. Res.*, *14*(3), 533–538, 1978.

Smith, R. E., D. L. Chery, Jr., K. G. Renard, and W. R. Gwinn, Supercritical flow flumes for measuring sediment-laden flow, *Tech. Bull. U.S. Dep. Agric.*, *1655*, 72 pp., 1981.

Topp, G. C., J. L. Davis, and A. P. Annan, Electromagnetic determination of soil water content: Measurements in coaxial transmission lines, *Water Resour. Res.*, *16*(3), 574–582, 1980.

Woolhiser, D. A., R. E. Smith, and D. C. Goodrich, KINEROS—A kinematic runoff and erosion model; documentation and user manual, *Publ. ARS-77*, 130 pp., Agric. Res. Serv., U.S. Dep. of Agric., 1990. (Available as *PB90-205-550* from Natl. Tech. Inf. Serv., Springfield, Va.)

Zegelin, S. J., I. White, and D. R. Jenkins, Improved field probes for soil water content and electrical conductivity measurement using time domain reflectometry, *Water Resour. Res.*, *25*(11), 2367–2376, 1989.

S. A. Amer, D. C. Goodrich, T. O. Keefer, and C. L. Unkrich, USDA ARS Southwest Watershed Research Center, 2000 East Allen Road, Tucson, AZ 85719.

L. B. Bach, USDA Forest Service, Pendleton, OR 97801.

T. J. Jackson, R. Parry, and T. J. Schmugge, USDA ARS Hydrology Laboratory, Beltsville, MD 20705.

(Received August 13, 1992; revised April 20, 1993; accepted October 19, 1993.)